Suppression of Alfvén Modes on the National Spherical Torus Experiment Upgrade with Outboard Beam Injection

E. D. Fredrickson,* E. V. Belova, D. J. Battaglia, R. E. Bell, N. A. Crocker, D. S. Darrow, A. Diallo, S. P. Gerhardt, N. N. Gorelenkov, B. P. LeBlanc, M. Podestà, and NSTX-U team

Princeton Plasma Physics Laboratory, Princeton, New Jersey 08543, USA and Department of Physics and Astronomy, University of California, Los Angeles, California 90095, USA

(Received 26 January 2017; revised manuscript received 7 April 2017; published 29 June 2017)

In this Letter we present data from experiments on the National Spherical Torus Experiment Upgrade, where it is shown for the first time that small amounts of high pitch-angle beam ions can strongly suppress the counterpropagating global Alfvén eigenmodes (GAE). GAE have been implicated in the redistribution of fast ions and modification of the electron power balance in previous experiments on NSTX. The ability to predict the stability of Alfvén modes, and developing methods to control them, is important for fusion reactors like the International Tokamak Experimental Reactor, which are heated by a large population of nonthermal, super-Alfvénic ions consisting of fusion generated α's and beam ions injected for current profile control. We present a qualitative interpretation of these observations using an analytic model of the Doppler-shifted ion-cyclotron resonance drive responsible for GAE instability which has an important dependence on $k_\perp \rho_L$. A quantitative analysis of this data with the HYM stability code predicts both the frequencies and instability of the GAE prior to, and suppression of the GAE after the injection of high pitch-angle beam ions.

DOI: 10.1103/PhysRevLett.118.265001

Introduction.—The National Spherical Torus Experiment (NSTX) and now the National Spherical Torus Experiment Upgrade (NSTX-U) [1] routinely operate with a super-Alfvénic fast ion population from neutral beam injection. This nonthermal population heats the thermal plasma, and is used to control the current profile to enhance plasma stability. However, the nonthermal fast ions also excite a broad range of instabilities, including global Alfvén eigenmodes (GAE) [2–6]. GAE are shear waves spatially localized near the minimum in the Alfvén continuum, with a frequency just below the minimum, $\omega < \omega_{\mathrm{Amin}} = \min[k_{||}(r)\, V_{\mathrm{Alfvén}}(r)]$. GAE have been implicated in electron thermal transport [7,8] and fast ion redistribution [9]. GAE are counterpropagating and excited through a Doppler-shifted cyclotron resonance [6]. The Doppler-shifted cyclotron resonance is also important in the interpretation of many astrophysical observations [10–12]. High frequency modes, also believed to have been excited through the Doppler shifted cyclotron resonance have also been seen in DIII-D [13]. In this Letter we will show that the addition of a small amount of nearly tangential fast ions ($V_{||}/V \approx 1$) can robustly suppress the GAE, both experimentally and in simulations with the HYM code. This damping mechanism is different than the use of sub-Alfvénic neutral beam ions to enhance the Landau damping of fusion-α-driven toroidal Alfvén eigenmodes on Tokamak fusion test reactor, stabilizing them until the beam injection was ended [14].

The new capability to control the fast ion distribution afforded by the new neutral beam sources on NSTX-U was key to demonstrating reliable suppression of the counter-propagating global Alfvén eigenmode. NSTX-U has six beam sources, the original three from NSTX with tangency radii inboard of the magnetic axis ($R_{\mathrm{mag}} \approx 1.1$ m) at $R_{\mathrm{tan}} \approx 0.7$, 0.6, and 0.5 m, (labeled 1a, 1b, 1c, respectively), and three new outboard sources with $R_{\mathrm{tan}} = 1.3$, 1.2, and 1.1 m (labeled 2a, 2b, 2c, respectively). A sketch of the neutral beam geometry is shown in Fig. 1. The green lines show the trajectories of the original, "inboard" neutral beam lines and the red lines show the trajectories of the new, "outboard" neutral beam lines. The approximate magnetic axis location for this shot ($R_{\mathrm{mag}} \approx 1.05$ m) is shown in black.

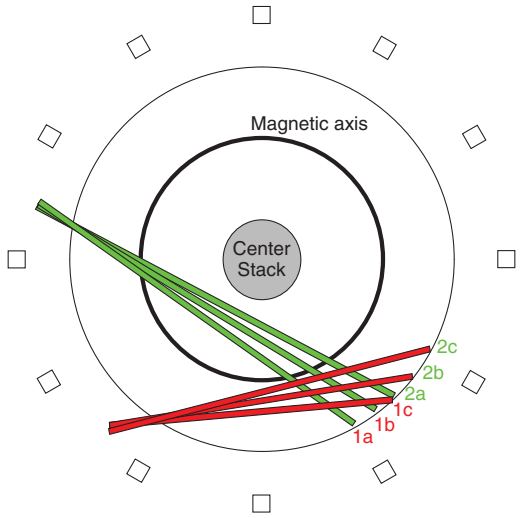

FIG. 1. Sketch of neutral beam geometry. Original NSTX beams in green, labeled 1a, 1b, 1c; new beams for NSTX-U shown in red labeled 2a, 2b and 2c.

 © 2017 American Physical Society

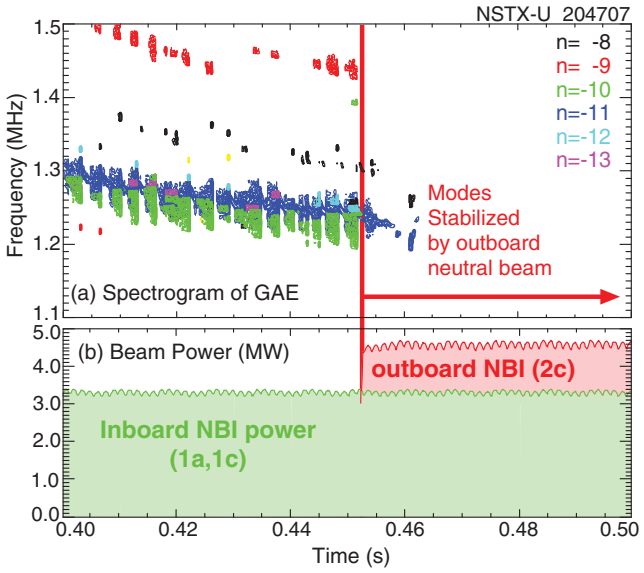

FIG. 2. (a) Color-coded spectrogram showing counterpropagating GAE activity. Dominant modes are $n = -10$ (green) and $n = -11$ (blue). (b) Green curve is inboard beam power, red curve is the off-axis beam power (source 2c).

All of the outboard neutral beams inject fast ions onto trajectories largely parallel to the magnetic field, thus with pitch, $0.8 < V_{\|}/V < 1$.

Suppression of GAE.—During the development of target plasmas in the initial commissioning of NSTX-U it was noticed that injection of any of the three new beam sources, with tangency radii larger than the radius of the magnetic axis, would effectively suppress the counterpropagating GAE. Figure 2 shows one of many examples where the addition of the new neutral beam source suppresses existing GAE. This is a 0.6 MA target plasma with a nominal 0.65 T toroidal field and, initially, two neutral beam sources injecting a total of 3.3 MW of heating power. The plasma density is peaked, with central density of $\approx 3.3 \times 10^{19}/\mathrm{m}^3$ and the peak electron and ion temperatures are ≈ 1.7 keV. The core rotation frequency is ≈ 28 kHz. A spectrogram of magnetic fluctuations from the toroidal array of Mirnov coils is shown in Fig. 2(a). The toroidal mode numbers are indicated by colors, with the dominant modes being $n = -10$ (green) and $n = -11$ (blue). There are also weaker $n = -8$, -9, -12, and -13 modes. The modes are propagating counter to the beam injection, toroidal rotation, and plasma current direction with a lab-frame frequency of ≈ 1.25 MHz at the analysis time of 0.44 s. The counterpropagation is consistent with a model predicting a Doppler-shifted cyclotron resonance (in the resonant beam ion frame, the mode frequency is equal to the ion cyclotron frequency). Correcting for the plasma rotation frequency, the mode frequency in the plasma frame is ≈ 1.5 MHz or $\approx 0.35\ f_{ci}$, thus the mode frequency is far from the thermal plasma ion cyclotron frequency.

At 0.45 s a third neutral beam source (2c) is added [Fig. 2(b), red curve], and the GAE are suppressed as can be seen in Fig. 2(a). The third neutral beam source adds only

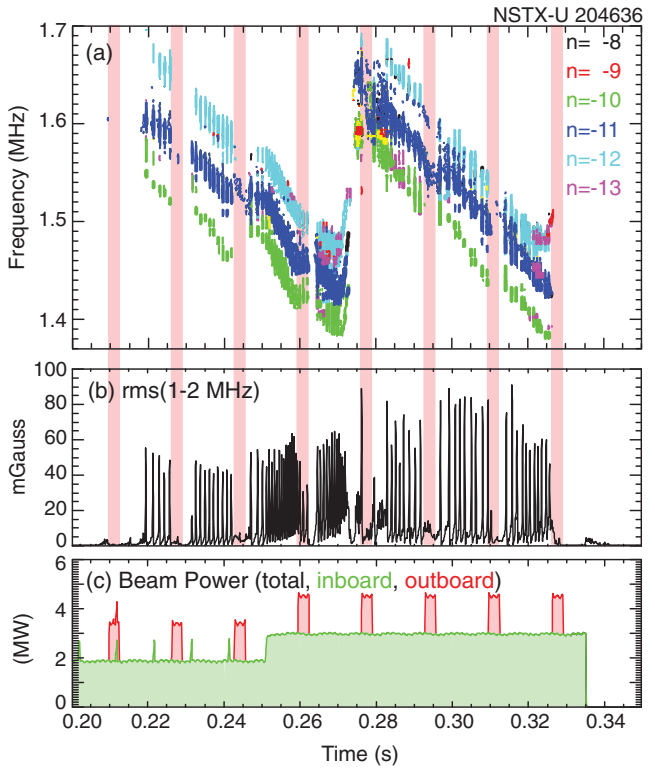

Fig. 3. (a) Color-coded spectrogram showing GAE activity. Dominant modes are $n = -10$ (green), $n = -11$ (blue), $n = -12$ (cyan). (b) rms amplitude of GAE, pink bars indicate when the outboard source is on. (c) Injected beam power, green is the total inboard source power, red shows outboard beam pulses (source 2b).

≈ 1.3 MW of additional heating power, making up $\approx 28\%$ of the total NBI heating power after 0.45 s. The suppression of GAE activity begins nearly simultaneously with the third source injection, on a time scale much shorter than the fast ion slowing down time of ≈ 25–50 ms. By 0.46 s, 8 ms after outboard source injection started, the neutron rate, a measure of the confined fast ion population, has increased $\approx 6\%$, confirming that a relatively small perturbation to the fast ion population can suppress the GAE.

The rapid suppression of the GAE is demonstrated more clearly in Fig. 3. In this shot a sequence of beam pulses with ≈ 3 ms duration are injected every 16 ms into a beam heated plasma with GAE activity. In Fig. 3(a) it is seen that the dominant modes are $n = -10$ (green), -11 (blue), and -12 (cyan). The secular variation in mode frequency, including the jump at 0.27 s, is consistent with the evolution of the inferred q profile (through $k_{\|}$) and plasma rotation through the Doppler frequency shift. The pink bars indicate when the 3rd source is on. Figure 3(b) shows the rms GAE amplitude showing bursting modes, similar in amplitude to the GAE bursts shown in Fig. 2. The bursts are completely suppressed with injection of the 3rd (outboard) source [Fig. 3(c)], with the exception of the fourth beam pulse during which there are two weaker GAE bursts. This clearly demonstrates that suppression can occur on a

millisecond time scale and that very few additional fast ions are needed to suppress the modes.

Theoretical analysis.—We can qualitatively understand the GAE suppression through an approximate dispersion relation for GAE and the Doppler-shifted ion cyclotron resonance condition, together with an analytic model of GAE stability [6]. We estimate $k_\parallel$ and $k_\perp$ from the GAE dispersion relation by evaluating the dispersion equation at the minimum of the continuum frequency, $\omega_{\mathrm{GAE}} \approx \min\{\mathrm{abs}[k_\parallel(r)\, V_{\mathrm{Alfvén}}(r) + |n|\omega_{\mathrm{rot}}(r)]\}$. Here ω_{GAE} is the measured mode frequency and $\omega_{\mathrm{rot}}(r)$ is the plasma rotation frequency. For the dominant $n = -11$ GAE, the continuum minimum is at $r_{\mathrm{min}} \approx 17$ cm ($R \approx 121$ cm). The Alfvén velocity at r_{min} is 1.38×10^8 cm/s and the plasma rotation frequency is ≈28 kHz, from which we find $k_\parallel \approx 0.070$ cm^{-1}. This $k_\parallel$ is fit with a poloidal mode number $m = -6$ giving $k_\perp = m/r \approx 0.36$ cm^{-1} (reflectometer array data shows $k_r \approx 0.08$ cm^{-1}). The resonance condition for fast ions is $\omega_{\mathrm{GAE}} + |k_\parallel \pm s/qR|V_{b\parallel} = \omega_{ci}$, with the strongest drive coming from the sideband resonances, $s = \pm 1$ [6]. The resonant parallel beam ion velocities for $s = \pm 1$ are $V_{b\parallel} \approx 2.26 \times 10^8$ and 2.68×10^8 cm/s.

The unperturbed fast ion distribution functions for the plasma shot shown in Fig. 2 are calculated with the TRANSP code at 0.44 and at 0.47 s, ≈10 ms before and ≈20 ms after the addition of the third source. The distribution functions averaged over the radial range $0.1 < r/a < 0.3$ are shown in Fig. 4. Comparison of Figs. 4(a) and 4(b) shows that the third neutral beam predominantly adds resonant fast ions with pitches greater than ≈0.9.

The fast ions satisfying the resonance condition are indicated in Figs. 4(a) and 4(b) by the solid black lines (only the lower $V_{b\parallel}$ curve intersects a significant fast ion population). The Doppler-shifted ion cyclotron resonance model predicts that for $k_\perp \rho_L < 1.9$, the resonant fast ions will be stabilizing, and destabilizing for $1.9 < k_\perp \rho_L < 3.9$, where ρ_L is the Larmor radius [6]. The blue dashed curve indicates where fast ions satisfy $k_\perp \rho_L \approx 1.9$. Resonant ions (black curves) with $\rho_L < 1/k_\perp \approx 5.4$ cm, will be stabilizing (i.e., along the black line and below blue dashed curve), resonant ions with $\rho_L > 5.4$ cm will be destabilizing (i.e., along the black line and above blue dashed curve). As can be seen by comparing Figs. 4(a) and 4(b), the injection of the outboard source adds more fast ions to the stabilizing part of the resonance curve (note that the stabilizing resonant fast density has increased by roughly a factor of 4).

The above analysis gives a qualitative explanation for the suppression of the $n = -11$ GAE. A more accurate analysis was done using the HYM stability code, using as input the experimental data and the fast ion parameters as calculated in the TRANSP code. The cyclotron resonance drive means that modeling the mode stability requires a code that uses a full orbit fast ion model. The HYM code [15–17] is an initial value, hybrid code in toroidal geometry which treats the beam ions using a full-orbit, delta-f particle

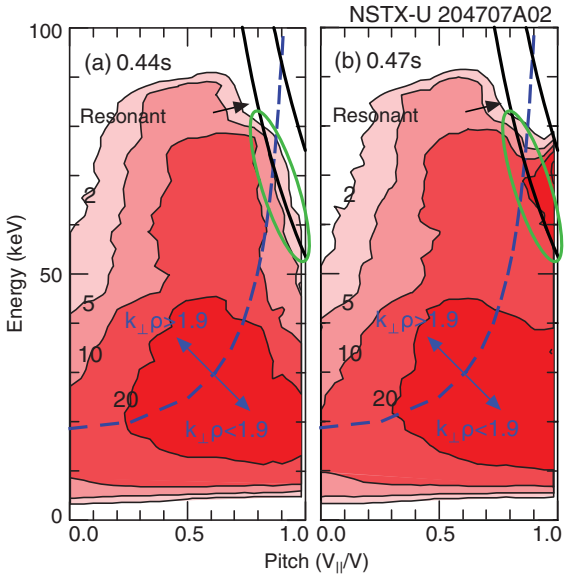

FIG. 4. TRANSP fast ion distributions for before and after the outboard beam injection. The dashed blue line indicates fast ions with $k_\infty \rho_L = 1.9$. Distribution functions are near the minimum of the continuum for the $n = -11$ mode. Contours are labeled in units of $10^7\ cn^{-3}\,\mathrm{eV}^{-1}\mathrm{dA}^{-1}$.

model. The background plasma is represented by one-fluid resistive magnetohydrodynamic model. The equilibrium fast ion distribution was input to HYM in the form $\mathrm{f}(\varepsilon, \lambda, \mathrm{p}_\varphi)$ as in Ref. [15], where $\lambda = \mu B_0/\varepsilon$ is a pitch parameter.

Simulations with the HYM code at 0.44 s find unstable GAE with $n = -7$ through -12 consistent with experiment [Fig. 5(a)]. The TRANSP pitch parameter distribution at $t = 0.44$ s was approximated by the function $\sim\exp[-(\lambda - \lambda_0)^2/\Delta\lambda^2]$, with $\lambda_0 = 0.7$, and $\Delta\lambda = 0.3$. The linear growth rates at 0.44 s for the modes are shown in Fig. 5(a), with the fastest growing modes being $n = -9$, -10, and -11 in good agreement with the experimental measurements. The mode frequencies are shown in Fig. 5(b) (red curve). HYM does not include the bulk toroidal rotation, so an approximate (small) Doppler correction is made to the simulated mode frequencies (blue curve) which results in good agreement with the experimental frequencies (blue asterisks). The modes magnetic fluctuations have shear polarization near the peak in-mode amplitude, showing that the modes found by HYM are in fact GAE and not compressional Alfvén eigenmodes.

In order to model an additional beam at $t = 0.47$ s, the distribution was modified to $\sim\exp[-(\lambda - \lambda_0)^2/\Delta\lambda^2] + 2\exp[-(1.5\lambda/\Delta\lambda)^2]$, which corresponds to adding a population of passing particles with $V_\parallel/V \sim 1$. A new equilibrium corresponding to the TRANSP run at $t = 0.47$ s has been calculated, including the modified beam contribution. A set of linearized simulations for $n = 7$–12 has demonstrated a complete stabilization of all modes for the $t = 0.47$ s case due to stabilizing effect of resonant particles with small λ.

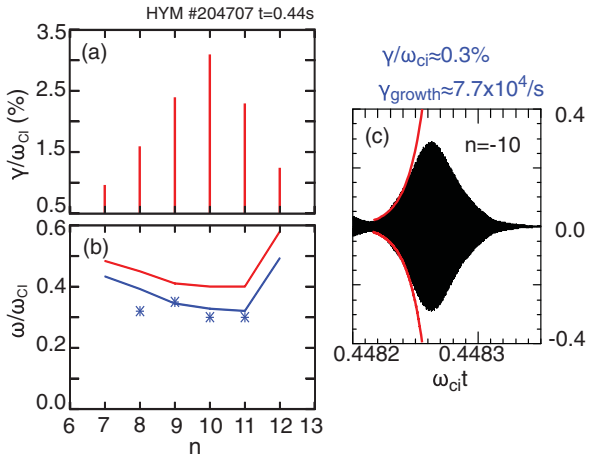

FIG. 5. (a) Growth rates and (b) frequencies of unstable counter-GAEs from HYM simulations for $t = 0.44$ s. Blue line is Doppler-shift corrected frequencies, points—experimental values, (c) GAE burst with fit to exponential growth (red).

Experimental estimates of the drive and damping rates for the GAE can be made from the growth and decay rates of the GAE bursts, Fig. 5(c). The bursts last for about 70 μs. The growth rate γ_{growth} of the burst is measured to be about 13 μs and the decay rate $|\gamma_{\text{decay}}|$ is about 16 μs. With the assumption that the damping rate is constant, and that the growth rate of the burst is $|\gamma_{\text{growth}}| \approx |\gamma_{\text{drive}}| - |\gamma_{\text{damp}}|$, and that $|\gamma_{\text{damp}}| \geq |\gamma_{\text{decay}}|$, then $\gamma_{\text{drive}} \geq |\gamma_{\text{growth}}| + |\gamma_{\text{decay}}|$. For comparison to the simulation results below, those numbers are normalized to the ion cyclotron frequency of $\approx 2.7 \times 10^7$ radians/s to get $\gamma_{\text{growth}}/\omega_{ci} \approx 0.3\%$ and $\gamma_{\text{drive}}/\omega_{ci} \approx 0.5\%$.

Summary.—Three neutral beam lines were added to the original three beam lines on NSTX during the recently completed upgrade from NSTX to NSTX-U. The new sources inject higher pitch-angle fast ions, allowing much greater flexibility in generating the fast ion distribution. In the first operational campaign on NSTX-U, the near tangential fast ions effectively suppressed the GAE. The GAE are one of the common beam driven instabilities seen on NSTX, and are correlated with enhanced core electron thermal transport. Analysis of one of these NSTX-U discharges with the HYM code at a time during strong GAE activity finds that the $n = -10$ and $n = -11$ counter-propagating GAE are most unstable, in good agreement with experimental measurements. HYM predicts that the GAE have strong growth rates of 2%–3% of the ion-cyclotron frequency. The predicted Doppler-corrected mode frequencies are between $0.3\,\omega_{ci}$ and $0.35\,\omega_{ci}$, in very good agreement with the observed mode frequencies. HYM simulations using the TRANSP fast ion distribution functions at 0.47 s, which is with an added population of fast ions with pitch greater than 0.9, find that the $n = -7$ through $n = -11$ modes are stable. The experimental results, HYM simulations, and analytic theory all suggest that stabilization is due to an increase in the population of high pitch, deeply passing particles with small Larmor radius which have a stabilizing effect on the GAEs. Further work is required to quantify the minimum required beam parameters sufficient for complete suppression of the instability. The agreement in unstable mode numbers and mode frequencies between theory and experiment in these initial results from the HYM code provide a strong validation of the HYM code physics, providing confidence in the use of HYM to predict stability of plasmas on the International Tokamak Experimental Reactor.

This work was supported by U.S. DOE Contracts No. DE-AC02-09CH11466 and DE-FG02-99ER54527.

*eric@pppl.gov

[1] M. Ono, J. Chrzanowski, L. Dudek *et al.*, Nucl. Fusion **55**, 073007 (2015).
[2] N. N. Gorelenkov and C. Z. Cheng, Nucl. Fusion **35**, 1743 (1995).
[3] K. Appert, R. Gruber, F. Troyon, and J. Vaclavik, Plasma Phys. **24**, 1147 (1982).
[4] V. S. Belikov, Y. I. Kolesnichenko, and R. B. White, Phys. Plasmas **10**, 4771 (2003).
[5] Y. I. Kolesnichenko, R. B. White, and Y. V. Yakovenko, Phys. Plasmas **13**, 122503 (2006).
[6] N. N. Gorelenkov, E. Fredrickson, E. Belova, C. Z. Cheng, D. Gates, S. Kaye, and R. White, Nucl. Fusion **43**, 228 (2003).
[7] D. Stutman, L. Delgado-Aparicio, N. Gorelenkov, M. Finkenthal, E. Fredrickson, S. Kaye, E. Mazzucato, and K. Tritz, Phys. Rev. Lett. **102**, 115002 (2009).
[8] E. V. Belova, N. N. Gorelenkov, N. A. Crocker, J. B. Lestz, E. D. Fredrickson, S. Tang, and K. Tritz, Phys. Plasmas **24**, 042505 (2017).
[9] E. D. Fredrickson, N. N. Gorelenkov, E. Belova, N. A. Crocker, S. Kubota, G. J. Kramer, B. LeBlanc, R. E. Bell, M. Podestà, H. Yuh, and F. Levinton, Nucl. Fusion **52**, 043001 (2012).
[10] J. V. Hollweg and P. A. Isenberg, J. Geophys. Res. **107**, 1147 (2002).
[11] M. Temerin and I. Roth, The production of ^{3}He, and heavy ion enrichments in ^{3}He-rich flares by electromagnetic hydrogen cyclotron waves, Astrophys. J. **391**, L105 (1992).
[12] C.-Y. Tu and E. Marsch, Aston. Astrophys. **368**, 1071 (2001).
[13] W. W. Heidbrink, E. D. Fredrickson, N. N. Gorelenkov, T. L. Rhodes, and M. A. Van Zeeland, Nucl. Fusion **46**, 324 (2006).
[14] Z. Chang *et al.*, Phys. Plasmas **4**, 1610 (1997).
[15] E. V. Belova, N. N. Gorelenkov, and C. Z. Cheng, Phys. Plasmas **10**, 3240 (2003).
[16] E. V. Belova, S. C. Jardin, H. Ji, M. Yamada, and R. Kulsrud Phys. Plasmas **7**, 4996 (2000).
[17] E. V. Belova, N. N. Gorelenkov, E. D. Fredrickson, H. L. Berk,G. J. Kramer, and S. S. Medley, *Proceedings of the 24th Int. Conf. San Diego, USA, 2012, paper TH/P6-16* (International Atomic Energy Agency, Vienna, 2012).